Int. J. Electrochem. Sci., 16 **(2021)** Article ID: 21099, doi: 10.20964/2021.09.28

International Journal of
ELECTROCHEMICAL
SCIENCE
www.electrochemsci.org

Fabrication of a Chitosan/Nitrogen Doped Carbon Sphere as Novel Electrochemical Sensor for the Detection of Rutin in Food Samples

Xingze Li

School of Materials Science and Engineering, Hubei Polytechnic University, Huangshi 435003, China
E-mail: lixingze_hb@163.com

Received: 3 May 2021 / *Accepted:* 1 July 2021 / *Published:* 10 August 2021

Flavonoid as a newly discovered nutrient, has essential physiological health effects on the human body. In this work, a very fast technique was proposed for the electrochemical analysis of rutin in food samples. Nitrogen-doped carbon nanospheres were synthesized for the surface modification of glassy carbon electrodes. The modified electrodes exhibited a sensitive response to rutin. After optimizations, this method can detect rutin in the range of 50 nM-10 μM, with the detection limit calculated to be 15.3 nM. In addition, the proposed electrochemical has been successfully adopted for detecting rutin in juice, pickled cucumbers and tomatoes.

Keywords: Flavonoids; Electrochemical sensor; Analytical method; Food samples; Nitrogen-doped carbon sphere

1. INTRODUCTION

Flavonoids are a class of yellow pigments derived from 2-phenyl chromogenic ketone as the basic parent nucleus structure, which also refer to a series of compounds with C_6-C_3-C_6 as the basic carbon frame [1–5]. According to the degree of oxidation of the three-carbon chain, the position of the B-ring connection and the possibility to form a ring with the three-carbon chain, major flavonoids can be divided into flavonoids, isoflavonoids, chalcones, anthocyanins and flavanones. Flavonoids are an important class of natural organic compounds, which is a class of secondary metabolites produced by plants in the process of long-term natural selection [6–10], and is widely found in the roots, stems, leaves, flowers and fruits of plants such as ginkgo biloba, kudzu root, soybean and other plants that are rich in flavonoids [11–13]. Different flavonoids vary in biological activities, among which the main physiological activities include anti-cancer effects, anti-cardiovascular disease, anti-osteoporosis,

elimination of free radicals, and antioxidant activities. Flavonoids also have a detoxifying effect on alcoholism and the treatment of alcohol dependence [14–16].

With the economic development of the food industry and the change of consumers' concept, healthy food containing natural active ingredients has become popular with modern people [17–23], among which flavonoids have received growing attention with the characteristics of pure nature, fast effect and high activity [24–29]. In recent years, research and clinical trials on propolis, tea polyphenols and ginkgo flavonoids have confirmed that flavonoids are both pharmacological factors and important nutritional factors. Flavonoid as a newly discovered nutrient, has an essential physiological health effects on the human body [30–33]. Flavonoids are widely found in plants, existing mostly in nature in the form of flavonoid glycosides and a few free sapogenins. Researchers are more concerned about extracting natural flavonoids with high purity and activity from plant bodies, and further processing them into health food or pharmaceutical products with specific functions such as anti-cancer, blood lipid regulation and anti-aging [34–38]. At present, in the development and application of health food, flavonoids are generally used in two ways, first of which is to directly apply the plant extract containing flavonoids to health food making and the other is to concentrate the plant extract containing flavonoids through a process of concentration, separation, purification, drying and other refining steps to produce high purity flavonoids [39–42].

In health food, the main applications are soy isoflavones, ginkgo flavonoid glycosides and Pueraria lobata isoflavones. Experiments have confirmed that soy isoflavones have bone resorption effect and can be used to regulate bone metabolism function. In addition, the health food with minerals, vitamins, etc. is particularly effective in the prevention of osteoporosis. These health food products benefit most for postmenopausal women, and can also be used as calcium supplements for young women. Ginkgo biloba flavonoid glycosides have positive effect in improving cerebral blood circulation and are used to prevent hypertension and arteriosclerosis. It is clinically reported that the total flavonoids of Pueraria lobata have been applied in lowering blood lipids, lowering blood pressure, preventing diabetes, cerebral atrophy, sudden deafness and even sobering up.

The detection of flavonoid in food should be preceded by appropriate processing, such as dehulling, crushing, grinding, homogenizing, etc., which include filtration, centrifugation, dissolution and purification, followed by digestion of the sample. The methods of digestion are usually dry ashing, wet digestion and closed digestion. The detection methods include atomic absorption spectrometry, graphite furnace atomic absorption, flame atomic absorption and inductively coupled plasma mass spectrometry [43]. However, these analytical methods often require large instruments and a long time of operation. In contrast, electrochemical sensors are much faster and simpler, which have been widely used in food detection [44–47], requiring sensitive detection electrodes. The preparation of suitable detection electrodes is the main research direction in this field.

Carbon nanosphere is one of the isomers of carbon in macroscopic level, and carbon nanosphere materials are spherical in microstructure, with their mechanical structure determining a high specific surface area, while their chemical composition determining its biocompatibility. Carbon nanosphere materials have a certain adsorption effect, a smaller size, and an ability to transfer electrons compared to other non-carbon materials. However, certain non-hydrophilic properties that are determined by the elemental composition and mechanical structure of carbon nanosphere materials greatly hinder their

application in aqueous systems. The doping of carbon nanomaterials with exotic elements can significantly improve their structure and electrical conductivity, among which nitrogen doping has become a heated research topic. Nitrogen is adjacent to carbon in the periodic table, and its atomic radius is close to that of carbon, thus the doping of nitrogen atoms can minimize the distortion of the original lattice of carbon materials. After being doped into carbon materials, nitrogen atoms play the role of loaded electrons, which increase the charge density of the materials, thus increasing the electrical conductivity. In this work, the glassy carbon electrode (GCE) was surface-modified with nitrogen-doped carbon nanospheres. Rutin has been used as sample of flavonoid in this work and the modified electrode was adopted to detect rutin in food samples. This sensor has been successfully applied to the detection of flavonoid in food in juice, pickled cucumbers and tomatoes.

2. MATERIALS AND METHODS

2.1. Preparation of nitrogen doped carbon spheres

20 mL of ethanol was mixed with 100 mL of water, and 1 mL of 1-butyl-3-methylimidazole hydroxide ionic liquid was added. The mixture was stirred for 2 h, after which 1 g of resorcinol and 0.8 mL of formaldehyde solution were added. The solution was stirred at room temperature overnight. Afterwards, the solution was transferred to a hydrothermal reactor and kept under 100°C for 12 h. After cooling process, the mixture was washed by water and ethanol, and dried at 100°C. The activation was conducted under a nitrogen atmosphere with 300°C for 3 h, after which the powder was carbonized in nitrogen atmosphere and heated up to 500°C at 1°C/min for 2 h. The final product was denoted as NC. A field emission scanning electron microscopy (SEM, ZEISS SUPRA 40VP) under secondary electron imaging mode was used for observing the morphology of the NC.

2.2. Electrode surface modification

The GCE was polished with 0.3 μm and 0.05 μm aluminum trioxide powder, and cleaned under sonication for 3 min. For GCE modification, NC dispersion (dispersed in a chitosan solution) was drop coated on the GCE surface and dried naturally. All electrochemical measurements were carried out in a CHI 760E working station. An Ag/AgCl (3M) and a Pt foil were adopted as reference electrode and counter electrode, respectively. The modified electrode was denoted as NC/GCE. Cyclic voltammetry and differential pulse voltammetry (DPV) have been applied to electrochemical characterization and sensing.

3. RESULTS AND DISCUSSION

Figure 1A shows the morphology of the prepared NC, from which it can be seen that the NC has uniform spheric shape. The nitrogen-doped carbon spheres are solid structures with smooth surfaces and

no impurities. The NC looks very similar to many previously synthesized carbon nanospheres [48,49]. The diameter size of the carbon nanospheres is very controllable, making them an ideal material for electrocatalysis. Based on the calculation of 200 individual particles, the average size of NC is at 120 nm (Figure 1B).

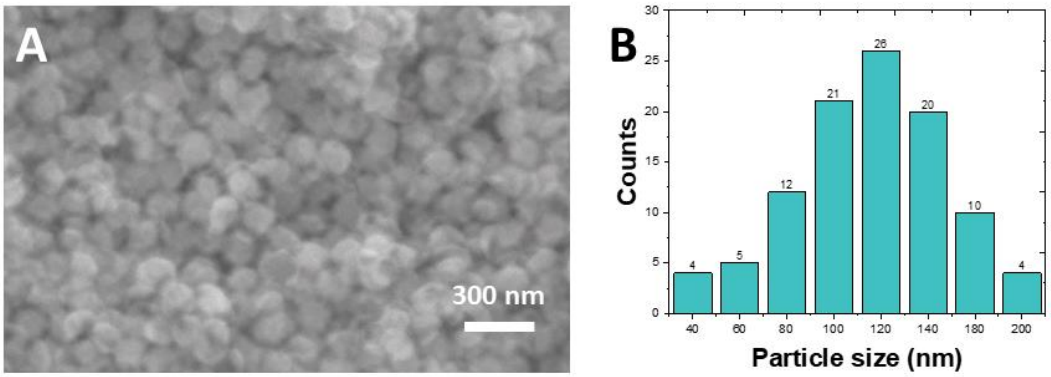

Figure 1. (A) SEM image and (B) size distribution of NC.

A preliminary test of GCE and NC/GCE was first conducted using B-R buffer (pH = 2) without other components. An appropriate amount of B-R buffer was added to the electrolytic cell for the test, and the working electrode was made of GCE and modified electrode. The reference electrode and auxiliary electrode were silver/silver chloride and platinum wire, respectively. The CV was conducted at the potential range from 0.2 to 0.8 V with a scan rate of 100 mV/s (Figure 2A). A comparative analysis of the electrochemical properties between the different working electrodes showed that the cyclic voltammetric current background of the NC/GCE in B-R buffer was larger than that of the GCE, indicating that its electrochemical sensitivity and electron transfer efficiency increased more significantly. Meanwhile, the presence of carbon nanospheres increased the surface area of the electrodes, which facilitated electrocatalytic sensing [50,51].

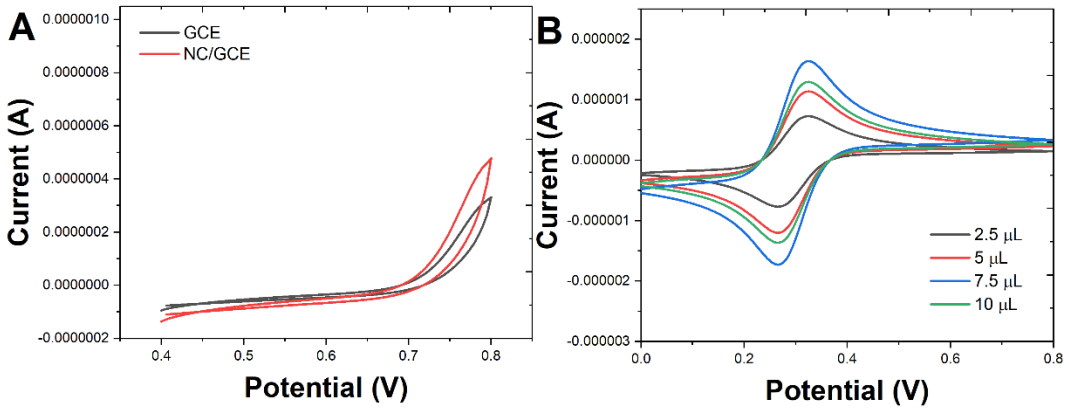

Figure 2. (A) CV of GCE and NC/GCE in B-R (pH=2). (B) CV of NC/GCE with different amount of NC towards 10 mM $K_3[Fe(CN)_6]$ solution (containing 0.1 M KCl). Scan rate: 50 mV/s.

To investigate the effect of coating amount on the electrochemical activity of NC/GCE, CV comparison tests in 2.5 mM of $[Fe(CN)_6]^{3-/4-}$ probe solution were performed after the modification of the electrode with different coating amounts. $[Fe(CN)_6]^{3-/4-}$ has been widely adopted as probe for analyzing the performance of electrode since they can provide a pair of largely distinct peaks [52–54]. The test performance is shown in Figure 2B, which presents that the magnitude of the peak current and the coating amount are positively correlated. However, the shape of the oxidation and reduction peaks deteriorated and when the coating amount was increased to 10 μL. It is possible that the dispersion was not evenly dispersed after drying, for the reason that the tension was affected by the excess coating amount on the working surface of the electrode. 7.5 μL is a suitable coating amount, which can form a stable water droplet on the surface of the electrode. Therefore, we set a coating amount of 7.5 μL for the electrode modification.

Rutin is commonly distributed in nature, which is mostly found in *Sophora japonica*, *Sophora angustifolia* and *Rutaceae brassicae* [55,56]. The current common techniques for the determination of rutin content include high performance liquid chromatography, spectrophotometry and capillary electrophoresis. However, HPLC is expensive and complicated to use, while the spectrophotometric methods are susceptible to interference but not highly sensitive. Electrochemical methods have the advantage of not destroying the sample when applied to flavonoids. Moreover, they can approach the ideal redox process of biomolecules under simulated conditions. Therefore, in this study, we have investigated the electrochemical performance and redox mechanism of rutin on NC/GCE by cyclic voltammetry.

First of all, the electrochemical behavior of rutin in Brittion-Robinson, $Na_2B_4O_7$-NaH_2PO_4, and NaAc-HAc buffers is investigated. The results showed that the strongest peak currents and distinct peak shapes were tested in B-R buffer with NC/GCE, thus B-R buffer was selected as the supporting electrolyte. The comparison of the CV performance of bare GCE and NC/GCE in blank B-R buffer for 1 μM rutin is shown in Figure 3, which reveals that the background current of NC/GCE increased but not significantly, while the electrochemical response to rutin was significantly enhanced. Both the oxidation and reduction peak currents of rutin solution were significantly increased, which indicates that the modification of NC can make the electrochemical sensitivity of GCE improved [57].

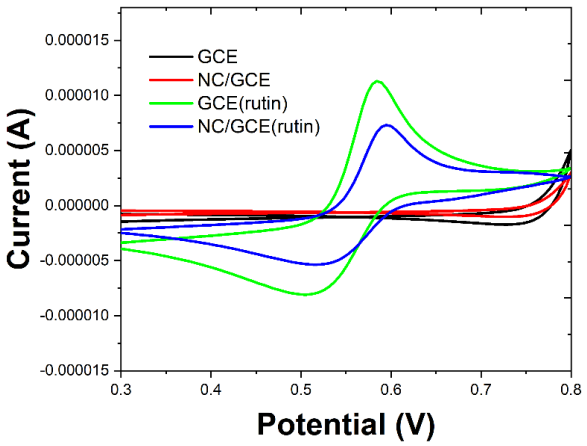

Figure 3. CV of GCE and NC/GCE in the presence or absence of 1 μM rutin recorded in B-R. Scan rate: 50 mV/s.

The CV test results for rutin solution with a concentration of 1 μM at various scan rates are shown in Figure 4. The magnitude of the oxidation peak current value and the scanning rate show a positive linear correlation, indicating that rutin is mainly controlled by the adsorption phenomenon on the working surface of NC/GCE. This result is highly consistent with the previous reports [58–61]. To further confirm the existence of adsorption, the NC/GCE was taken out and rinsed with water and placed directly into the blank B-R buffer for the same scanning. As a result, oxidation and reduction peaks appeared, but the current of the peaks became smaller, indicating the presence of adsorption under rutin on the NC/GCE surface.

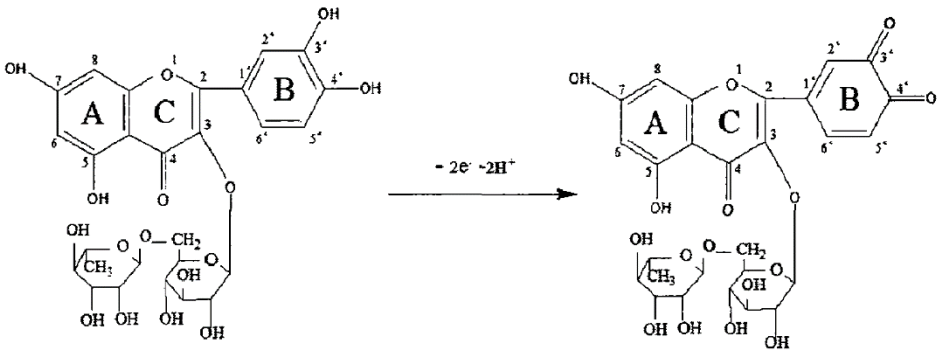

Figure 4. The oxidation process of hydroxyl groups on rutin B ring.

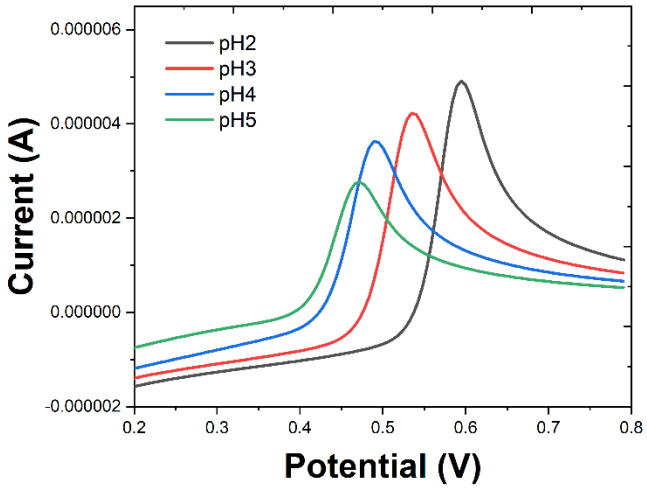

Figure 5. DPVs of 1 μM rutin at B-R buffer of different pH condition. 0). Amplitude: 50 mV; Pulse width: 0.05 s; Pulse period: 0.5 s.

The results presents that the magnitude of the oxidation and reduction peak currents became larger with the increase of the scanning speed, while the ratio of the redox peak currents tended to become smaller. The increase in scanning speed led to a larger potential difference between the oxidation and reduction peak potentials, indicating that the redox process of rutin on the NC/GCE surface is a quasi-reversible reaction. Based on the above experimental results, it could be determined that the redox

process of rutin in the tested system is quasi-reversible, involving two electrons and two protons. It can also be assumed that the oxidation and reduction peak currents are generated by the reaction of the hydroxyl groups at the 3' and 4' positions of the rutin B ring (Figure 5).

Figure 5 shows the performance of 1 μM rutin in a differential pulse voltammetry (DPV) in B-R buffer at a range of pH values. As presented in the figure, rutin in B-R buffer exhibited a good electrochemical oxidation peak shape. With the increase of pH, the oxidation peak potential shifts negatively and the peak current decreases, thus a negative linear correlation exists between the magnitude of peak potential and the magnitude of pH. According to the slope complex formula of the Nernst equation, the slope of the isoelectron transfer is 60.25, which indicates that the oxidation reaction of rutin in the experimental system involves equal electrons and protons. The B-R buffer with pH 2 was selected as the electrolyte solution in the subsequent experiments on a comprehensive consideration.

Table 1. The detection limit of rutin in different reference.

Sensor	LR	LOD	Reference
GR/CILE	70 nM-10 μM	24 nM	[62]
GR–AuNPs/CSPE	100 nM-15 μM	11 nM	[63]
IL/CPE	40 nM-10 μM	10 nM	[64]
MWCNTs–CHIT/ABPE	20 nM-10 μM	10 nM	[65]
NC/GCE	50 nM-10 μM	15.3 nM	This work

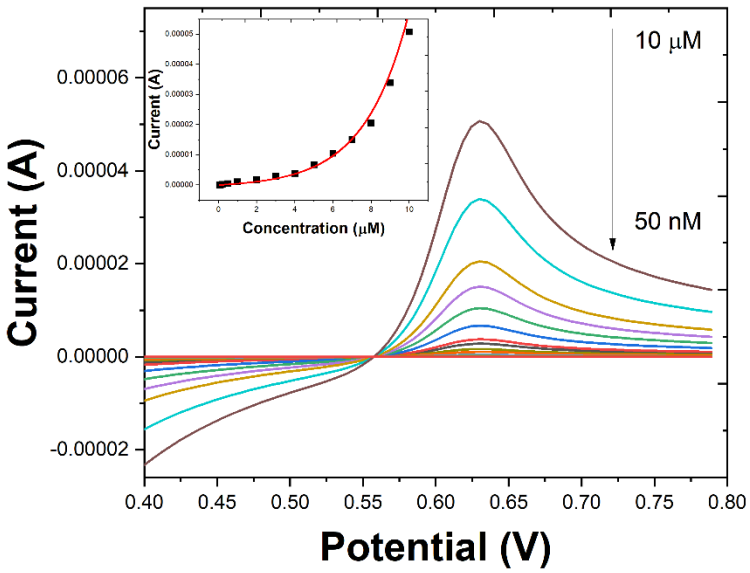

Figure 6. DPVs of NC/GCE towards different concentrations of rutin in B-R. Amplitude: 50 mV; Pulse width: 0.05 s; Pulse period: 0.5 s. Inset: calibration curves.

After optimizing all parameters, the linear detection range of the sensor was investigated. As shown in Figure 6, the current value increases with the concentration of rutin. The linear detection curve of the NC/GCE sensor for runtin is shown in Figure 6, which presents that there is a favorable linear

relationship between NC/GCE in the range of 50 nM-10 μM. The equation was: $y = 4.21461E^{-7}*\exp(-x/-2.18801) + 4.21461E^{-7}*\exp(-x/-2.67423) + -8.56248E^{-7}$. As shown in Table 1, the detection limit was calculated as 15.3 nM and the detection limits of rutin obtained in this work meet the requirements of low detection limits, indicating that NC/GCE can effectively detect rutin.

Selectivity is one of the most essential parameters for electrochemical sensors. For the purpose of investigating the selectivity of NC/GCE, the sensor first detected the electrochemical signal of a solution with a concentration of 1 μM rutin, and added other metal ions with different concentrations as shown in Figure 7, which presents that NC/GCE has a positive selectivity and can be used for the detection of complex systems.

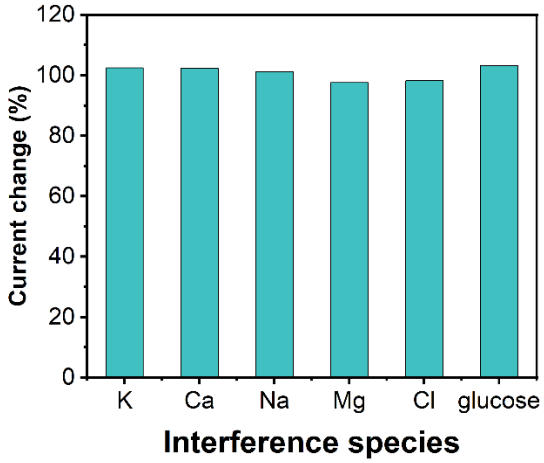

Figure 7. Selectivity performance of the NC/GCE for rutin detection (interference species: K^+, Ca^{2+}, Na^+, Mg^{2+}, Cl^-, glucose).

Aiming to investigate the feasibility of NC/GCE in actual sample detection, a standard recovery method was adopted to detect the content of rutin in juice, pickled cucumbers and tomatoes. As shown in Table 2, the recovery of NC/GCE was within the range of 94.0-104.0%, indicating that NC/GCE can be used for the detection of food samples with high accuracy.

Table 2. Determination of rutin in food samples using NC/GCE (n=3).

Sample	Added (μM)	Detected (μM)	Recovery rate (%)
Juice 1	0.00	0.00	-
Juice 2	0.50	0.47	94.0
Pickled cucumber 1	0.00	0.00	-
Pickled cucumber 2	1.00	1.04	104.0
Tomato 1	0.00	0.42	-
Tomato 2	2.00	2.35	97.1

4. CONCLUSION

In conclusion, nitrogen-doped carbon nano was synthesized for the surface modification of GCE and this NC/GCE has a very sensitive response to the detection of rutin. After optimization, the NC/GCE can provide linear detection of rutin in the range of 50 nM-10 μM. The detection limit was calculated to be 15.3 nM. This electrochemical sensor has excellent anti-interference performance. The NC/GCE has been successfully adopted for the detection of rutin in juice, pickled cucumbers and tomatoes.

References

1. S. Kubendhiran, R. Sakthivel, S.-M. Chen, Q.-J. Yeah, B. Mutharani, B. Thirumalraj, *Inorg. Chem. Front.*, 5 (2018) 1085–1093.
2. K. Zhu, T. Lv, T. Qin, Y. Huang, L. Wang, B. Liu, *Chem. Commun.*, 55 (2019) 13983–13986.
3. B.T. Ferrara, E.P. Thompson, *Biotechniques*, 66 (2019) 65–71.
4. L. Fu, Z. Liu, J. Ge, M. Guo, H. Zhang, F. Chen, W. Su, A. Yu, *J. Electroanal. Chem.*, 841 (2019) 142–147.
5. W. Wu, Q. Zhou, Y. Zheng, L. Fu, J. Zhu, H. Karimi-Maleh, *Int J Electrochem Sci*, 15 (2020) 10093–10103.
6. C.-C. Huang, W. Chen, *Microchim. Acta*, 185 (2018) 1–8.
7. M. He, H. Wu, J. Nie, P. Yan, T.-B. Yang, Z.-Y. Yang, R. Pei, *J. Pharm. Biomed. Anal.*, 146 (2017) 37–47.
8. F. Wang, L. Chen, H. Chen, S. Chen, Y. Liu, *Molecules*, 24 (2019) 2680.
9. L. Fu, Y. Zheng, P. Zhang, H. Zhang, M. Wu, H. Zhang, A. Wang, W. Su, F. Chen, J. Yu, W. Cai, C.-T. Lin, *Bioelectrochemistry*, 129 (2019) 199–205.
10. Q. Liu, Y. Zheng, L. Fu, B.A. Simco, C.A. Goudie, *Aquaculture*, 532 (2021) 735952.
11. M. Elmastaş, A. Demir, N. Genç, Ü. Dölek, M. Güneş, *Food Chem.*, 235 (2017) 154–159.
12. J. Zhou, Y. Zheng, J. Zhang, H. Karimi-Maleh, Y. Xu, Q. Zhou, L. Fu, W. Wu, *Anal. Lett.*, 53 (2020) 2517–2528.
13. L. Fu, A. Wang, G. Lai, W. Su, F. Malherbe, J. Yu, C.-T. Lin, A. Yu, *Talanta*, 180 (2018) 248–253.
14. J. Chen, Z. Yuan, H. Zhang, W. Li, M. Shi, Z. Peng, M. Li, J. Tian, X. Deng, Y. Cheng, *J. Exp. Bot.*, 70 (2019) 2759–2771.
15. A. Özkan, *Fresenius Environ. Bull.*, 29 (2020) 143–151.
16. A. El-Bindary, Z. Anwar, T. El-Shafaie, *J. Mol. Liq.*, 323 (2021) 114607.
17. L. Corell, S. Armenta, F.A. Esteve-Turrillas, M. de la Guardia, *Microchem. J.*, 140 (2018) 74–79.
18. Z. Zhao, S. He, Y. Hu, Y. Yang, B. Jiao, Q. Fang, Z. Zhou, *Sci. Hortic.*, 224 (2017) 93–101.
19. F. Kizilgeci, N.E.P. Mokhtari, A. Hossain, *Fresenius Environ. Bull.*, 29 (2020) 8592–8599.
20. L. Fu, Y. Zheng, P. Zhang, H. Zhang, Y. Xu, J. Zhou, H. Zhang, H. Karimi-Maleh, G. Lai, S. Zhao, W. Su, J. Yu, C.-T. Lin, *Biosens. Bioelectron.*, 159 (2020) 112212.
21. W. Wu, M. Wu, J. Zhou, Y. Xu, Z. Li, Y. Yao, L. Fu, *Sens. Mater.*, 32 (2020) 2941–2948.
22. L. Fu, W. Su, F. Chen, S. Zhao, H. Zhang, H. Karimi-Maleh, A. Yu, J. Yu, C.-T. Lin, *Bioelectrochemistry* (2021) 107829.
23. X. Zhang, R. Yang, Z. Li, M. Zhang, Q. Wang, Y. Xu, L. Fu, J. Du, Y. Zheng, J. Zhu, *Rev. Mex. Ing. Quím.*, 19 (2020) 281–291.
24. O. Ozbek, O. Gokdogan, M.F. Baran, *Fresenius Environ. Bull.*, 30 (2021) 1125–1133.
25. I. Bolat, A. Ikinci, *Fresenius Environ. Bull.*, 29 (2020) 1542–1549.
26. D. Bojilov, S. Dagnon, I. Ivanov, *Phytochem. Lett.*, 20 (2017) 316–321.
27. L. Fu, Q. Wang, M. Zhang, Y. Zheng, M. Wu, Z. Lan, J. Pu, H. Zhang, F. Chen, W. Su, *Front. Chem.*, 8 (2020) 92.

28. L. Fu, K. Xie, D. Wu, A. Wang, H. Zhang, Z. Ji, *Mater. Chem. Phys.*, 242 (2020) 122462.
29. R. Yang, B. Fan, S. Wang, L. Li, Y. Li, S. Li, Y. Zheng, L. Fu, C.-T. Lin, *Micromachines*, 11 (2020) 967.
30. P. Kuppusamy, K.D. Lee, C.E. Song, S. Ilavenil, S. Srigopalram, M.V. Arasu, K.C. Choi, *Rev. Bras. Farmacogn.*, 28 (2018) 282–288.
31. Z. Demir, D. Işık, *Fresenius Environ. Bull.*, 29 (2020) 1974–1987.
32. L. Fu, Y. Zheng, P. Zhang, J. Zhu, H. Zhang, L. Zhang, W. Su, *Electrochem. Commun.*, 92 (2018) 39–42.
33. Y. Zheng, Y. Huang, H. Shi, L. Fu, *Inorg. Nano-Met. Chem.*, 49 (2019) 277–282.
34. E. Knoch, S. Sugawara, T. Mori, R. Nakabayashi, K. Saito, K. Yonekura-Sakakibara, *Planta*, 247 (2018) 779–790.
35. P. Shi, W. Du, Y. Wang, X. Teng, X. Chen, L. Ye, *Food Sci. Nutr.*, 7 (2019) 148–154.
36. G. Liu, X. Yang, H. Zhang, L. Fu, *Int J Electrochem Sci*, 15 (2020) 5395–5403.
37. J. Ying, Y. Zheng, H. Zhang, L. Fu, *Rev. Mex. Ing. Quím.*, 19 (2020) 585–592.
38. M. Zhang, B. Pan, Y. Wang, X. Du, L. Fu, Y. Zheng, F. Chen, W. Wu, Q. Zhou, S. Ding, *ChemistrySelect*, 5 (2020) 5035–5040.
39. A.A. Abdullah, Y. Yardım, Z. Şentürk, *Talanta*, 187 (2018) 156–164.
40. C. Veith, M. Drent, A. Bast, F. van Schooten, A. Boots, *Toxicol. Appl. Pharmacol.*, 336 (2017) 40–48.
41. Y. Zheng, J. Zhu, L. Fu, Q. Liu, *Int J Electrochem Sci*, 15 (2020) 9622–9630.
42. Y. Xu, Y. Lu, P. Zhang, Y. Wang, Y. Zheng, L. Fu, H. Zhang, C.-T. Lin, A. Yu, *Bioelectrochemistry*, 133 (2020) 107455.
43. K. Gopalasatheeskumar, G.A. Kumar, T. Sengottuvel, V.S. Devan, V. Srividhya, *Asian J. Res. Chem.*, 12 (2019) 335–337.
44. H. Karimi-Maleh, Y. Orooji, F. Karimi, M. Alizadeh, M. Baghayeri, J. Rouhi, S. Tajik, H. Beitollahi, S. Agarwal, V.K. Gupta, *Biosens. Bioelectron.* (2021) 113252.
45. H. Karimi-Maleh, F. Karimi, S. Malekmohammadi, N. Zakariae, R. Esmaeili, S. Rostamnia, M.L. Yola, N. Atar, S. Movaghgharnezhad, S. Rajendran, A. Razmjou, Y. Orooji, S. Agarwal, V.K. Gupta, *J. Mol. Liq.*, 310 (2020) 113185.
46. H. Karimi-Maleh, M. Alizadeh, Y. Orooji, F. Karimi, M. Baghayeri, J. Rouhi, S. Tajik, H. Beitollahi, S. Agarwal, V.K. Gupta, S. Rajendran, S. Rostamnia, L. Fu, F. Saberi-Movahed, S. Malekmohammadi, *Ind. Eng. Chem. Res.*, 60 (2021) 816–823.
47. H. Karimi-Maleh, A. Ayati, R. Davoodi, B. Tanhaei, F. Karimi, S. Malekmohammadi, Y. Orooji, L. Fu, M. Sillanpää, *J. Clean. Prod.*, 291 (2021) 125880.
48. J.-G. Wang, H. Liu, H. Sun, W. Hua, H. Wang, X. Liu, B. Wei, *Carbon*, 127 (2018) 85–92.
49. H. Tian, J. Liang, J. Liu, *Adv. Mater.*, 31 (2019) 1903886.
50. L. Liu, H. Zhao, L. Shi, M. Lan, H. Zhang, C. Yu, *Electrochimica Acta*, 227 (2017) 69–76.
51. J. Qian, D. Zhang, L. Liu, Y. Yi, M.N. Fiston, O.J. Kingsford, G. Zhu, *J. Electrochem. Soc.*, 165 (2018) B491.
52. Z. Cheng-Jun, M. Xiong-Hui, L. Jian-Ping, *Chin. J. Anal. Chem.*, 45 (2017) 1360–1366.
53. Y. Liu, Y. Liang, R. Yang, J. Li, L. Qu, *Talanta*, 195 (2019) 691–698.
54. S. Yu, M. Mehrgardi, C. Shannon, *Electrochem. Commun.*, 88 (2018) 24–28.
55. Y. Lu, J. Hu, Y. Zeng, Y. Zhu, H. Wang, X. Lei, S. Huang, L. Guo, L. Li, *Sens. Actuators B Chem.*, 311 (2020) 127911.
56. R. Xing, X. Zhao, Y. Liu, J. Liu, B. Liu, Y. Ren, S. Liu, L. Mao, *J. Nanosci. Nanotechnol.*, 18 (2018) 4651–4657.
57. N.K. Swamy, K.N.S. Mohana, M.B. Hegde, A.M. Madhusudana, K. Rajitha, S.R. Nayak, *J. Appl. Electrochem.*, 51 (2021) 1047–1057.
58. L. Lu, L. Wu, W. Wang, X. Long, J. Xu, H. He, *Int J Electrochem Sci*, 13 (2018) 2126–2135.
59. A. Şenocak, A. Khataee, E. Demirbas, E. Doustkhah, *Sens. Actuators B Chem.*, 312 (2020)

127939.
60. J. Wang, B. Yang, S. Li, B. Yan, H. Xu, K. Zhang, Y. Shi, C. Zhai, Y. Du, *J. Colloid Interface Sci.*, 506 (2017) 329–337.
61. M.L. Yola, C. Göde, N. Atar, *J. Mol. Liq.*, 246 (2017) 350–353.
62. F. Gao, X. Qi, X. Cai, Q. Wang, F. Gao, W. Sun, *Thin Solid Films*, 520 (2012) 5064–5069.
63. I. Apetrei, C. Apetrei, *Measurement*, 114 (2018) 37–43.
64. Y. Zhang, J. Zheng, *Talanta*, 77 (2008) 325–330.
65. P. Deng, Z. Xu, J. Li, *J. Pharm. Biomed. Anal.*, 76 (2013) 234–242.